A Circuit-Equivalent Battery Model Accounting for the Dependency on Load Frequency

Yukai Chen
Politecnico di Torino
Email: yukai.chen@polito.it

Enrico Macii
Politecnico di Torino
Email: enrico.macii@polito.it

Massimo Poncino
Politecnico di Torino
Email: massimo.poncino@polito.it

***Abstract*—Circuit-equivalent battery models are considered de-facto standard for modeling and simulation of digital systems due to many practical advantages. In spite of the many variants of models proposed in the literature, none of them accounts for one important feature of the battery dynamics, namely, the dependency on the *frequency* of current load profile. For a given average current value, current loads with different spectral distributions may have quite different impacts on the battery discharge. This is a very well-know issue in the design of hybrid energy storage systems, where different types of storages devices are used, each with different storage efficiency for different load frequency ranges.**

We propose a basic modification to a state-of-the-art model that incorporates this load frequency dependency, as well as a methodology to identify the frequency-sensitive parameters of the model from publicly available data (e.g., datasheets). The results show that frequency-agnostic models can significantly overestimate the battery state-of-charge, and that this effect is far from being negligible.

I. Introduction

The ubiquity of battery-power devices has made models of batteries an essential component of electronic system simulators; the humongous variety of models available in the literature is driven by different needs by designers belonging to different application domains and with different backgrounds [1].

In the context of electronic design, users typically need basic feedback about a battery, e.g., the discharge time and/or its state-of-charge (SOC) for a given load profile. Although these effects can be tracked by different types of models, electronic designers tend to favor models in which the battery dynamics is mimicked by an equivalent electrical circuit [2]–[4], for their easy integration within existing EDA environment.

State-of-the-art circuit equivalent models are reasonably accurate for providing such high-level information, and are able to track the most relevant battery non-idealities. However, these models tend to priviledge accurate *tracking of the dynamics of the output voltage* rather than the effect of these non-idealities on battery SOC. The main reason for this is that the most basic information in co-simulating a battery and a device is the *lifetime of the battery*, defined as the time in which the output voltage reaches a specific value (the *cutoff voltage*).

However, in many applications, it is important also to accurately track *the battery SOC*, for example to drive custom battery management policies. The model of [3], which has become quite popular if not a standard in the domain of low-power digital design, does not model the effect that current load dynamics have **on the battery SOC**. By current dynamics we mean in particular (i) the variance (i.e., variation across the average value), and (ii) the frequency (i.e., the spectral characteristics) of the load frequency. In practice, [3] yields the same SOC profile for any load current waveform with a given average value. Due to the (non-linear) dependency of battery voltage on SOC, this is equivalent to say that the discharge time is not affected by the current dynamics.

While the former issue (the variance) is taken into account in other similar models (e.g., [5]), the issue of load frequency has never been considered so far in battery models. However, this is a very well-know issue to be considered when designing *hybrid* energy storage systems, where different types of energy storages devices (ESDs) are used. Hybridization is introduced precisely because different ESDs have different "response" to current loads with different frequencies.

To address this issue, we propose a basic modification to the model of [3] that incorporates this sensitivity to load frequency. Besides the model itself, one important contribution also includes as a methodology to identify the frequency-sensitive parameters of the model from publicly available data (e.g., datasheets).

Results show that frequency-agnostic models such as [3] can significantly overestimate the battery state-of-charge, and that this effect is far from being negligible.

II. Background and Related Work

A. Background

In this work we focus only on the effects of load current dynamics on the battery discharge. Other important, yet second-order, effects such as battery capacity loss and/or temperature-related effects are out of the scope of this work.

A well-known non-ideality of a battery is the *rated capacity* effect [4], i.e., the fact that the usable capacity of a battery depends on the magnitude of the discharge current: at larger currents, a battery is less efficient in converting its chemically stored energy into electrical energy. Rated capacity effect normally refers to constant discharge currents, since datasheets usually report discharge curves for different *current values*. Nevertheless, usable capacity is also affected by the *variance*

978-3-9815370-8-6/17/$31.00

of the current profile; among all possible current waveforms with a given average value, a constant current will result in the largest equivalent capacity [6].

Some models also include the so-called *recovery effect*, i.e., the fact that batteries have some recovery capacity when discharge periods are interleaved with rest periods. We do not consider recovery in our models since recent experiments show how it is somehow overrated, especially in Li-Ion cells [7].

The empirical, circuit-equivalent model of [3] shown in Figure 1 is widely used in the electronic design domain because its relative accuracy and simplicity. The circuit consists of

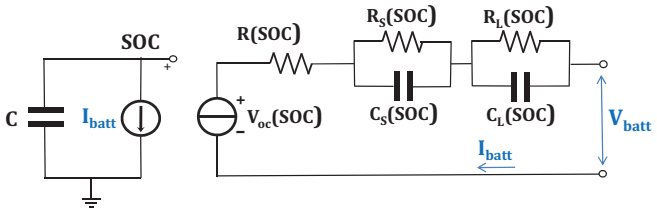

Figure 1. The reference circuit equivalent template [3].

two main sections. The left one includes a capacitor C (representing the nominal battery capacity in Ah) and a current generator modeling the load current I_{batt}. The voltage across the capacitor tracks the SOC of the battery (node SOC).

In the right branch of the model, a voltage-controlled voltage generator expresses the non-linear dependence of battery open-circuit voltage V_{oc} on SOC. The RC network models the battery impedance, by exposing a series resistance $R(SOC)$ that models the internal resistance of the battery, and two RC blocks tracking the the short- (R_S, C_S) and long-term (R_L, C_L) time constants of a step response; all these parameters are, in the most general scenario, function of the SOC.

B. Tracking Load Current Dynamics

The model of Figure 1 can track the battery voltage V_{batt} over time; thanks to the RC network in the right side it will yield different V_{batt} waveforms for load current profiles with different dynamics. As an example, consider the plot in Figure 2, showing V_{batt} for two loads, one with a constant 500mA discharge (solid), and a second one (dashed) for a square wave with same average value but a 50% duty cycle and voltage levels of 800mA/200mA from 0s to 1000s, then it ends with same average constant value. The model refers to a CGR18650CG battery by Panasonic [8].

However, when it comes however to tracking the SOC (the voltage node in the left side), it is evident that the constant current generator I_{batt} on the left side will result in only small differences between the two workloads since the average value is the same. Figure 3 shows the SOC for the same two workloads of Figure 2. The dashed curve (duty-cycled waveform) is indeed different from the constant one, but this is mostly due to the temporal order of the two current levels. In

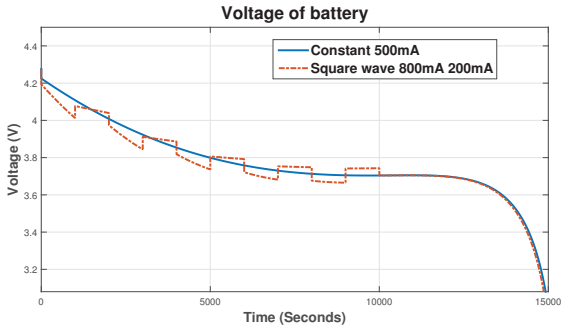

Figure 2. Battery voltage for two workloads with same average value using the model of [3].

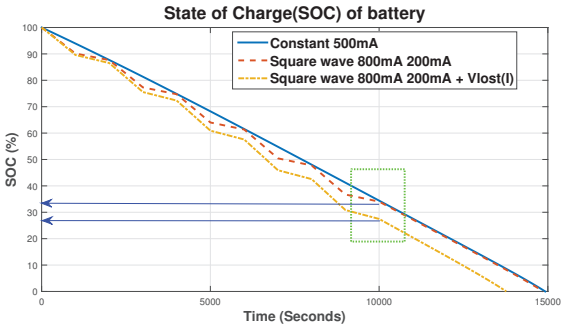

Figure 3. SOC for the workloads of Figure 2 using the model of [3].

practice the dashed curve is a linear piece-wise approximation of the constant discharge. As a matter of fact, the two curves intersect at the end of each period. At the time point enclosed in the rectangle, the two SOC curves coincide, which is not the expected behavior. An important consequence of this fact is that, since V_{oc} is a function of SOC, such insensitivity to current dynamic will also be reflected on the battery voltage.

This issue has been addressed by other models in the literature, in particular the one of [5], in which this dependency was accounted by adding a voltage generator $V_{lost}(I_{load})$ in series to the left part of the model (Figure 4), which reduces the available charge of the battery (which in turn controls V_{oc}) and is in general a non-linear function of the discharge rate. With

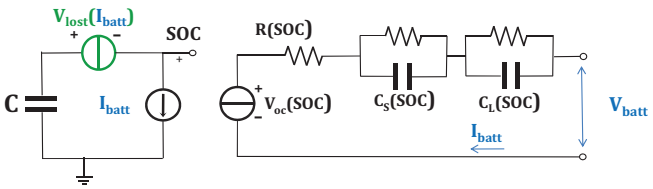

Figure 4. Adding the dependency of capacity (SOC) on load current in the model of [3].

this addition, the SOC will be affected in a more pronounced way by a larger current than for a smaller one. This is reflected by the dash-dot curve of Figure 3. It is evident how the actual SOC is consistently lower than what tracked by the model of

[3]. This lower SOC will also be reflected onto V_{oc}, which will consequently also modify the voltage discharge curve.

The model of Figure 4 will be our baseline model for the extension proposed in our work.

III. Adding Load Frequency Sensitivity

Although more accurate for SOC tracking, the model of Figure 4 cannot distinguish between the two workloads shown in Figure 5. They have the same average value I_{avg}, the same current swing $[I_m, I_M]$ and duty cycle, and only differ in their frequency, with the load of Figure 5-(a) having a frequency $f_1 = 1/T_1$ roughly half of that of Figure 5-(b) ($f_2 = 1/T_2$).

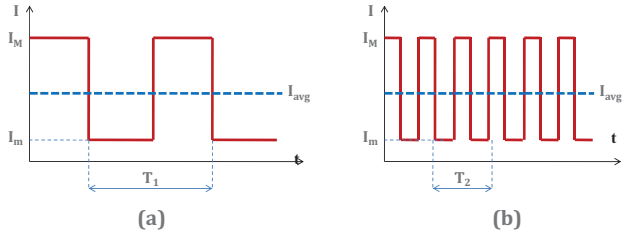

Figure 5. Two current workloads with different frequencies.

The model of Figure 4 cannot track the different frequency of the two workloads because it subtracts, at each time interval, an amount of SOC dependent on load current in that interval $V_{lost}(I_{batt})$, which is the same for both waveforms. Indeed, it is intuitive that the higher frequency load on the right will stress the battery more, since the chemical reactions will occur at a higher rate.

This dependency on load frequency is somehow underrated in the design of electronic system; however, this effect is not negligible. This is a very well-know issue in the design of *hybrid* energy storage systems, where different types of energy storages devices (ESDs) are used because of their different "response" to current loads with different frequencies. This fact is visually represented by the popular Ragone chart [9], which plots energy densities (i.e., the available energy per unit weight) vs. power density (the speed at which the energy can be drawn). The traditional Ragone chart (an example is shown in Figure 6) typically displays broad categories of ESDs (e.g., batteries, supercapacitors), as *regions* in the plane (rectangles in the figure). Empirical method to derive a *curve* in the Ragone space are discussed in the literature [10].

Discharge rates are specified in C-rate, which by definition also correspond to a *discharge time* (e.g., 1C rate correspond to discharging the battery in 1 hour). By using the inverse of the discharge time as the load frequency [11], we can interpret Ragone curves as a behavior of a battery capacity vs. the frequency of current load [10], [12]. The Ragone chart clearly shows that any ESD has some preferred frequency range. In the case of batteries, they can easily manage load with frequencies in the 1Hz-0.2mHz range [12].

Such dependency between capacity and load frequency can be incorporated into the model of Figure 4 using a similar

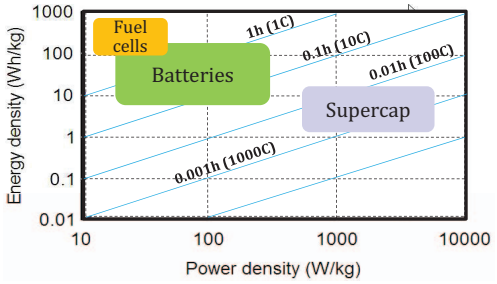

Figure 6. Ragone Chart: Energy density vs. Power density of Various ESDs.

structure as for the $V_{lost}(I_{batt})$; the resulting model is shown in Figure 7, where the load frequency dependence is modeled by adding an extra voltage generator $V_{lost}(f_{load})$ in the left mesh of the circuit, which will cause a voltage drop (i.e., a loss of SOC) depending on the frequency of the current load.

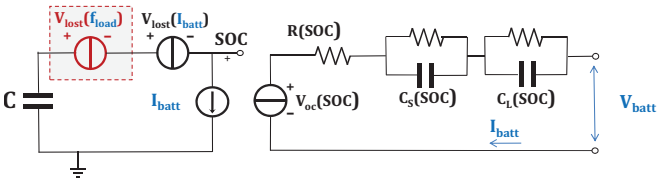

Figure 7. Battery model incorporating frequency dependence.

The following section will describe how to identify the parameters of the models and how to use the model at runtime, in particular for what concerns the frequency-dependent behavior.

IV. Methodology

The identification of the parameters of the model in Figure 1 is addressed in previous works, and can be done either by measurements [3] or by resorting to public data from datasheets [13], [14]. We need to discuss only how to determine the values corresponding to the two V_{lost} voltage generators in the model of Figure 7. In order to also derive these two additional elements we adopt the datasheet-based approach of [13], [14] which, thanks to its generality, allows us to model different batteries with limited effort and reasonable accuracy.

A. Extracting $V_{lost}(I_{batt})$ and $V_{lost}(f_{load})$

Both voltage generators in Figure 7 can be computed from a single type of information that is provided by virtually any battery of any chemistry, namely the Voltage vs. Capacity (or SOC) curves. Figure 8 shows an example of these curves for a popular cylindric Li-Ion battery, namely the CGR18650CG by Panasonic(nominal voltage of 3.6V, 2250 mAh capacity, and cutoff voltage of 2.5V) [8].

The process to derive the relations between the lost capacity with respect to current and frequency from a set of V vs. C(or SOC) is described in [10]. This method allows deriving the

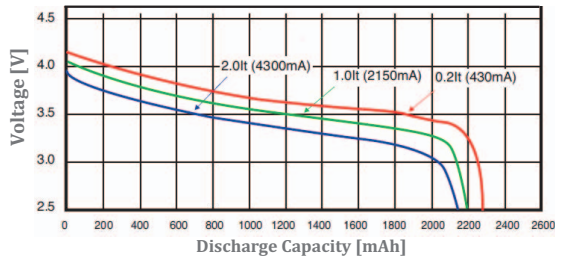

Figure 8. Discharge Curves for the example Panasonic Battery.

relation between battery capacity vs. load current ($C(I_{batt})$ and load frequency ($C(f_{load})$.

Given these two functions, their translation into a variation of the SOC (implemented in the circuit as a voltage drop through the voltage generators) is carried out as follows.

$V_{lost}(I_{batt})$ is derived by computing, at each simulation time step Δt, the following equation:

$$\Delta SOC(I_{batt}) = \frac{I_{Batt} \times \Delta t}{C(I_{batt})} - \frac{I_{Batt} \times \Delta t}{C_{nom}} \quad (1)$$

where $C(I_{Batt})$ is relationship between capacity and battery current derived from datasheet as described above and C_{nom} is the nominal capacity as in the datasheet. Notice that since I_{batt} in principle changes at each Δt, the ΔSOC is updated in each time step.

The calculation of $V_{lost}(f_{load})$ is a bit more articulated, since the frequency of the current load is not an instantaneous quantity during simulation. In principle, the spectral characteristics of the load should be computed on the entire load waveform, which is obviously incompatible with a runtime evaluation of the model. This is however a known issue in spectral analysis and can be easily solved by analyzing the load waveform over shorter time intervals. In practice, we define a time window and extract the spectral characteristics over this window. Although many approaches are possible, we use the Short Time Fourier Transform (STFT) to compute load frequency components in each window. STFT is used to determine frequency information for non-stationary signals and simply consists of computing the Fourier transform separately on each segment. thus allowing to determine the spectrum as a function of time, which is what we need for our purpose.

$V_{lost}(f_{load})$ is obtained by evaluating Equation 2 at each Δt.

$$\Delta SOC(f_{load}) = \sum_{i=1}^{N_{FFT}} \left(\frac{I_{Batt}(i) \times \Delta t}{C(f_{load})} - \frac{I_{Batt}(i) \times \Delta t}{C_{nom}}\right) \quad (2)$$

N_{FFT} is length of timing window in STFT; $I_{Batt}(i), i = 1, \ldots, N_{FFT}$ is a string of current values within a timing window; $C(f_{load})$ is by relation between capacity and load frequency extracted from datasheet.

The value of f_{load} to be used in the model in a given timing window is determined by calculating the *dominating frequency* components in the STFT. This is done by first deriving the *energy spectral density* function (i.e. the distribution of the frequency components); from this function we derive its cumulative distribution $\mathbf{F}_{f_{load}}(f)$, which indicated what percentage of the spectrum has frequencies $\leq f$. The *dominant frequency* is defined as the value of f that includes the 90% of the entire spectrum, as done in [10].

V. Simulation Results

A. Simulation Setup

For proving the effectiveness of our proposed battery model, we designed a system described in SystemC-AMS, consisting of (i) a Li-ion rechargeable battery, (ii) a load, modeled as current and voltage waveforms over time, and (iii) a DC-DC converter connecting the battery to the load, modeled as in [16] and whose conversion efficiency is function of input voltage, output voltage and current.

We chose two popular Lithium-ion batteries, namely, Panasonic UR16650ZT [15] and CGR18650CG [8], and derived the proposed model for both batteries. Table I summarizes the battery parameters; their datasheets provide enough information to derive all model parameters of Figure 1. We then extracted the two functions of capacity used the method of [10]. Empirical fitting of these functions yields the relation listed in Equations 3–6. Equations 3 and 4 refer to UR16650ZT, while Equations 5 and 6 to the CGR18650CG.

Then, as described in Section IV, we translated these two functions in the corresponding $V_{lost}(I_{batt})$ and $V_{lost}(f_{load})$.

Parameters	UR16650ZT	CGR18650CG
Rated Capacity	2200mAh	2250mAh
Nominal Voltage	3.7V	3.6V
Weight	41.0g	45.0g
Cut-off voltage	3.0V	2.5V

Table I
Manufacture parameters of Selected batteries

$$C(I_{batt}) = -542.6 \times I_{batt}^{1.165} + 7920 \quad (3)$$
$$C(f_{load}) = -1.102 \times e^{-6} \times f_{load}^{0.8045} + 7920 \quad (4)$$
$$C(I_{batt}) = -290.8 \times I_{batt}^{1.084} + 8100 \quad (5)$$
$$C(f_{load}) = -3.921 \times e^{-6} \times f_{load}^{1.058} + 8100 \quad (6)$$

B. Load Current Value Effect

We first illustrate the effect of load current value on battery capacity used model is shown in Figure 4, and eventually add frequency dependency.

For this simulation, we use a squared wave of frequency $0.5mHz$, 50% duty cycle, average value 800mA, two different swing values ($\pm 300mA$ and $\pm 500mA$). Simulation results are shown in Figures 9 and 10 for different batteries. We can observe a discharge time of 1156s (13.4% shorter than that of constant current simulated with model in Figure 1) for UR16650ZT and 581s (6.4%) for CGR18650CG for the smaller swing; and 1751s (20.3%) for UR16650ZT and 797s (8.7%) for CGR18650CG for the larger one. The differences due to the different swings are 595s (6.9%) for the UR16650ZT and 216s (2.3%) for the CGR18650CG.

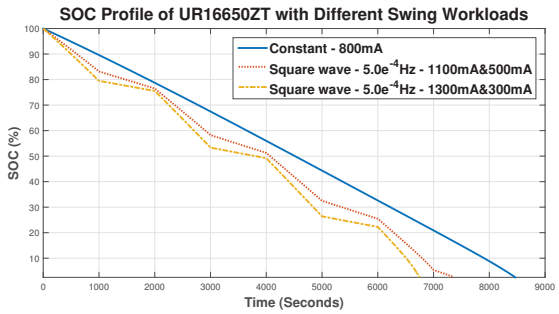

Figure 9. Load current effect for different workloads of UR16650ZT.

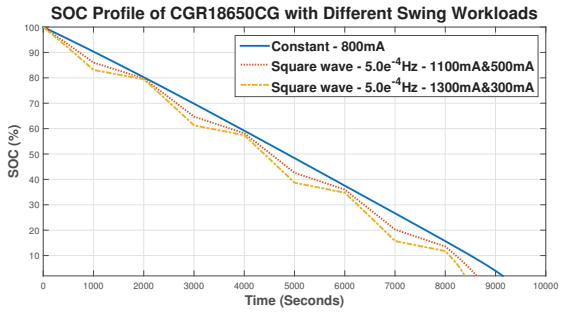

Figure 10. Load current effect for different workloads of CGR18650CG.

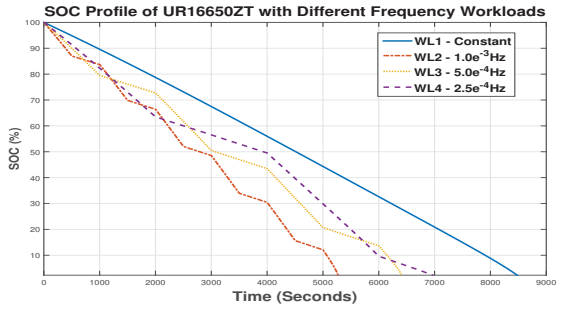

Figure 11. Load frequency effect for different workloads of UR16650ZT.

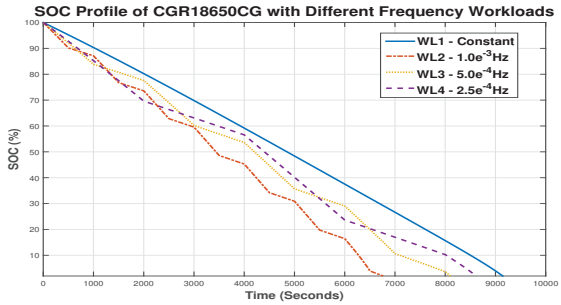

Figure 12. Load frequency effect for different workloads of CGR18650CG.

C. Load Frequency Effect

We now include the the effect of load frequency in the model as in Figure 7. We simulate three square waves with same average current value (800mA) and swing values ($\pm$ 300mA), but different frequencies and compare to a constant workload (WL1) has the same average current used model in Figure 1 as a reference. Table II summarizes the frequencies of workloads we used.

Workload	WL1	WL2	WL3	WL4
Frequency	–	$1mHz$	$0.5mHz$	$0.25mHz$

Table II
FREQUENCY OF SYNTHETIC WORKLOADS

Figure 11 and 12 show SOC profile simulation results of the two chosen batteries. It is clearly shown in the plots that the lifetime of battery decreases with increased load frequency. Concerning battery UR16650ZT, the difference of discharge time between constant workload and $1mHz$ frequency workload is 3216s; in terms of battery CGR18650CG, such difference is 2258s. It reveals that battery UR16650ZT is more sensitive to load frequency than CGR18650CG. This is also due to a smaller capacity and a higher cutoff voltage.

In order to evaluate the added contribution of the frequency dependence, we compare WL3 of Figure 11 and 12 with the plot of same workload in Figures 9 and 10, which has same load frequency and load current profile. We can notice that the 0% SOC is reached at 7345s/8621s (for the two batteries) when considering only load current, but this time reduces to 6398s/8086s when including the dependency on load frequency(11.0% and 6.2% shorter than only considering load current for the two batteries).

D. Simulation with Real Workloads

We used our example EES to execute two different real workloads (Figure 13) corresponding to different set of tasks and different power management options, yet with similar average currents (432.8 mA vs. 429.1 mA). The workloads are obtained by simulating a system-level description of the SoC and represent 5 hours of activity.

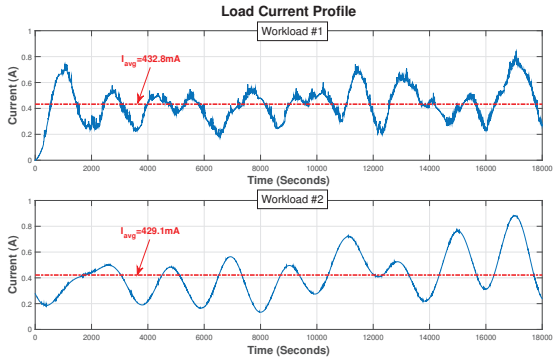

Figure 13. Two example real workloads.

Figure 14 shows the frequency spectrogram of the two workloads as computed by STFT, by setting the timing window to 32. The frequency spectrums clearly show the different frequency components in the two workloads (e.g., compare the initial part of the trace, in which Workload # 1 is more intensively using relatively higher frequencies than #2).

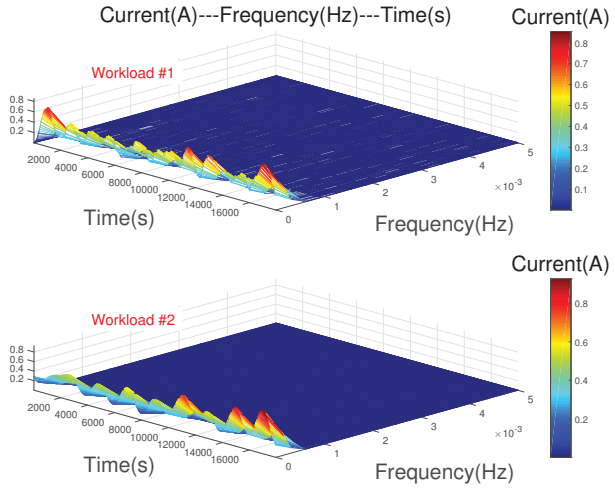

Figure 14. Spectrogram of the two workloads of Figure 13.

In order to observe the load frequency effect on battery capacity, we used same average current value constant load as reference to compare the difference in discharge time. Results are shown in Figures 15 and 16. For both batteries, the difference in discharge time between constant and real workload is bigger for workload #1 than for #2 due to relatively higher frequency components of #1 than workload #2, as observed from the spectrogram of Figure 14.

Concerning the difference between these two batteries, we found that the difference for CGR18650CG is smaller than that of UR16650ZT for both workloads, showing again that the UR16650ZT is more sensitive to load frequency.

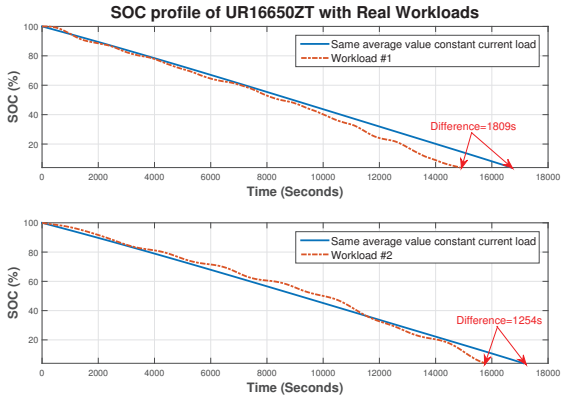

Figure 15. SOC profile of UR16650ZT with Real Workloads.

VI. Conclusions

We have presented a method to include the dependency of a battery on the spectral characteristics of a current load, and the relative electrical circuit-equivalent model for the simulation for this effect. The model is empirically derived from very basic data provided in most datasheets, and its usage on synthetic and real workloads show that this effect is underrated in current state-of-the-art models.

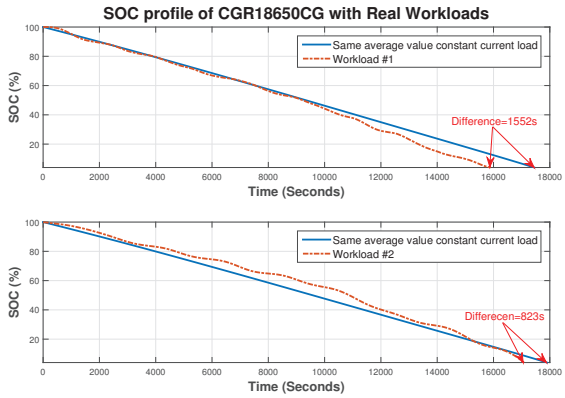

Figure 16. SOC profile of CGR18650CG with Real Workloads.

Besides its conventional use as an accurate tracker of the battery SOC and/or discharge time, another relevant application of this model can be for sizing of a hybrid energy storage system; for instance, to quickly evaluate different combinations of, say, a hybrid battery-supercapacitor configuration.

References

[1] R. Rao, S. Vrudhula, D. N. Rakhmatov, "Battery modeling for energy aware system design," *IEEE Computer*, Vol. 36 , No. 12, pp. 77–87.

[2] M. C. Glass, "Battery electrochemical nonlinear/dynamic SPICE model," in *Proc. IEEE Energy Conversion Engineering Conference*, 1996, pp. 292–297.

[3] M. Chen and G. Rincón-Mora, "Accurate electrical battery model capable of predicting runtime and IV performance," *IEEE Transactions on Energy Conversion*, vol. 21, no. 2, pp. 504–511, 2006.

[4] D. Linden and T. Reddy, *Handbook of batteries*. McGraw-Hill, 2002.

[5] Benini, Luca, et al. "Discrete-time battery models for system-level low-power design," *IEEE Transactions on Very Large Scale Integration (VLSI) Systems*, vol. 9, no. 5, pp. 630–640, 2001.

[6] P. Rong, M. Pedram, "An analytical model for predicting the remaining battery capacity of lithium-ion batteries," *IEEE Transactions on VLSI Systems*, Vol. 14, No. 5, pp. 441-451, 2005.

[7] Narayanaswamy, Swaminathan, et al. "On battery recovery effect in wireless sensor nodes," *ACM Transactions on Design Automation of Electronic Systems*, Vol. 21, No. 4, 2016.

[8] Panasonic UR16650ZT datasheet, http://www.meircell.co.il/files/Panasonic\%20CGR18650CG.pdf

[9] D. V. Ragone, "Review of battery systems for electrically powered vehicles." No. 680453. *SAE Technical Paper,* 1968.

[10] C. Yukai, E. Macii, M. Poncino, "Frequency domain characterization of batteries for the design of energy storage subsystems," *International Conference on Very Large Scale Integration,* IEEE, 2016.

[11] A. Kuperman, I. Aharon, A. Kara, S. Malki, "A frequency domain approach to analyzing passive battery-ultracapacitor hybrids supplying periodic pulsed current loads." *Energy Conversion and Management* 52.12 (2011): 3433-3438.

[12] E. M. Krieger, "Effects of variability and rate on battery charge storage and lifespan." http://arks.princeton.edu/ark:/88435/dsp01x633f110k

[13] N. K. Medora, A. Kusko, "Dynamic battery modeling of lead-acid batteries using manufacturers' data," *INTELEC'05*, 2005.

[14] Petricca, Massimo, et al. "An automated framework for generating variable-accuracy battery models from datasheet information," *Proceedings of the 2013 International Symposium on Low Power Electronics and Design,* IEEE Press, 2013.

[15] Panasonic CGR18650CG datasheet, https://na.industrial.panasonic.com/sites/default/pidsa/files/ur16650zt.pdf

[16] A. Park, Y. Wang, Y. Kim, N. Chang, M. Pedram, "Battery management for grid-connected PV systems with a battery," *Proceedings of the 2012 ACM/IEEE international symposium on Low power electronics and design,* ACM, 2012.